JOURNAL OF VIROLOGY, Feb. 1996, p. 1163–1172 Vol. 70, No. 2
0022-538X/96/$04.00+0

SR Protein Splicing Factors Interact with the Rous Sarcoma Virus Negative Regulator of Splicing Element

LISA M. MCNALLY AND MARK T. MCNALLY*

Department of Microbiology, Medical College of Wisconsin, Milwaukee, Wisconsin 53226

Received 24 April 1995/Accepted 15 November 1995

Retroviral replication requires that a portion of the primary transcripts generated from proviral DNA be spliced to serve as mRNA for the envelope protein and in Rous sarcoma virus as *src* mRNA. However, a substantial amount of full-length RNA must be maintained in an unspliced form, as the unspliced RNA serves both as mRNA for structural proteins and virion-associated enzymatic proteins and as genomic RNA for progeny virions. The extent of viral RNA splicing must be finely controlled, since only a narrow range in the ratio of unspliced RNA to spliced RNA is tolerated for optimal replication. A number of *cis*-acting sequences within the RNA of Rous sarcoma virus play a role in preserving a large pool of unspliced RNA. One such sequence, the negative regulator of splicing (NRS), is of interest because it blocks splicing but is not located near any of the splice junctions. To better understand how this novel element blocks splicing at a distance, we set out to identify host cell factors that interact specifically with this inhibitory sequence. In this study, proteins from nuclear extracts with molecular masses of 26, 36, 44, and 55 kDa were shown by UV cross-linking assays to bind the NRS preferentially. One of them, p55, was also detected in a specific complex identified in an electrophoretic mobility shift assay. All but p55 have biochemical properties consistent with SR protein splicing factors, and some, but not all, of the total SR proteins purified from HeLa cells cross-link specifically to the NRS. The strongest cross-linking SR protein is SRp30a/b, which is composed of the splicing factors SF2/ASF and SC35. The NRS specifically binds bacterially expressed SF2/ASF, whereas nonfunctional mutants do not. Data indicating that the 36-kDa protein which cross-links in nuclear extracts is SF2/ASF are presented. The data indicate that factors normally required for RNA splicing may be exploited by retroviruses to block splicing.

Incomplete splicing of primary RNA transcripts is a common feature of retroviral replication (8). The full-length RNA synthesized from the proviral DNA is capped and polyadenylated and can be transported efficiently to the cytoplasm, where it serves as mRNA for structural and enzymatic proteins and as genomic RNA for progeny virions. A portion of the primary transcripts serves as precursor for RNA splicing in the nucleus to generate subgenomic mRNAs encoding, in the simplest cases, the envelope protein which is expressed on the surface of the virus and interacts with host cell receptors to initiate infection. Despite the requirement of splicing for viability, a surprisingly large fraction of the retroviral RNA remains unspliced (50 to 80%). All members of the retrovirus family depend on the host splicing apparatus for generation of spliced RNA, and since host cell RNAs are generally spliced to completion, it follows that a mechanism(s) to control viral RNA splicing exists (41). Complex retroviruses like human immunodeficiency virus and human T-cell lymphotropic viruses encode auxiliary proteins that can influence RNA metabolism at various levels to facilitate cytoplasmic accumulation of incompletely spliced RNA (10). Inefficient splicing and RNA transport in simpler viruses like Rous sarcoma virus (RSV) seem to be mediated by *cis*-acting RNA signals only, rather than through an alteration of the splicing-transport apparatus, since these viruses don't encode regulatory proteins and viral RNAs are correctly processed even in the absence of viral protein synthesis (41).

* Corresponding author. Mailing address: Department of Microbiology, Medical College of Wisconsin, 8701 Watertown Plank Rd., Milwaukee, WI 53226. Phone: (414) 456-8749. Fax: (414) 266-8522. Electronic mail address: mtm@post.its.mcw.edu.

One of the simple retroviruses, RSV, contains a single 5′ splice site that can be joined to one of two alternative 3′ splice sites to generate the *env* and *src* mRNAs (Fig. 1). Several laboratories have identified *cis*-acting signals that suppress either the overall level of splicing or splicing to one of the alternative 3′ splice sites. One signal coincides with the *env* 3′ splice site region and was first identified by Katz et al. (22), who found that insertion of an oligonucleotide upstream of the *env* 3′ splice site resulted in a marked increase in *env* mRNA. It was shown that the oligonucleotide fortuitously generated an improved branch point sequence that resulted in increased *env* splicing in vivo and in vitro (14, 23). Inefficient use of the RSV *env* 3′ splice site was confirmed for other viral constructs (6) and for heterologous RNAs containing the *env* 3′ splice site paired with the 5′ splice site of a cellular gene (29). Thus, the env 3′ splice site is maintained in a suboptimal form. A second signal resides near the *src* splice site. Deletion of sequences from position −189 to position −166 relative to the *src* 3′ splice site resulted in increased splicing to *src*, but not *env*, and indicated the presence of an element that negatively influences *src* splicing specifically (6). Heterologous RNAs containing the *src* 3′ splice site region could be efficiently spliced only when this upstream element was missing (29). This element is distinct from the *src* splice site, and the mechanism by which it functions to suppress *src* splicing remains unclear, although it has been shown to involve a factor unique to chicken cells (3). A recent study also indicated that the pyrimidine tract associated with the *src* 3′ splice site is suboptimal (47). A third element, termed the negative regulator of splicing (NRS), has a global negative effect on RSV RNA splicing and resides in the *gag* gene, approximately 300 nucleotides (nt) from the 5′ splice site and more than 4,000 nt from the *env* 3′ splice site (4,

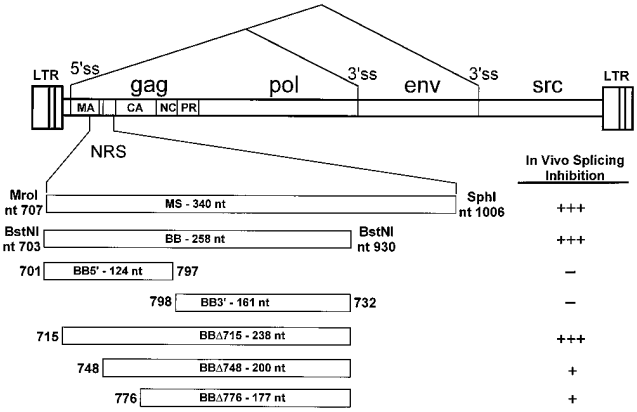

FIG. 1. RSV provirus structure and genome positions of the NRS RNAs used in this study (not to scale). Shown are the long terminal repeats (LTR); *gag*, *pol*, *env*, and *src* genes; and the splices necessary to generate subgenomic RNAs (lines between the 5′ and 3′ splices [5′ss and 3′ss]). The NRS region is indicated in reference to the matrix (MA) and capsid (CA) genes, and the boxes below represent the different in vitro transcripts with the endpoints of the NRS on the outside and the transcript names and their sizes in nucleotides (including polylinker sequences) on the inside. The relative NRS in vivo splicing inhibition activities on the right were reported previously (31), except that for BBΔ715, which was determined for this study. Steady-state levels of unspliced RNA are indicated as follows: −, 0 to 10% unspliced (levels obtained with no insert); +, 11 to 30% unspliced; ++, 31 to 50% unspliced; and +++, 51 to 80% unspliced.

31). In contrast to the former cases, mutations in the NRS effect a coordinate increase in *env* and *src* splicing. All three signals appear to be necessary for optimal replication, since more efficient splicing leads to decreased pools of unspliced RNA and even a modest decrease in the level of unspliced RNA leads to impaired replication (22, 47). Presumably, the decreased level of genome and *gag-pol* mRNA causes the replication defect.

Some progress has been made toward understanding the mechanism of NRS splicing inhibition. The NRS was manifest as an oversplicing phenotype in proviral constructs harboring certain *gag* deletions, and this phenotype was not corrected by reinsertion of NRS fragments in the antisense orientation (4, 42). The findings that the NRS blocks splicing of heterologous RNAs in an orientation-dependent manner and influences only the intron containing it in two intron constructs (31) suggested that the NRS affects splicing directly and that the observed increase in the level of spliced RNA was not the result of perturbation of some other processing event such as RNA stability or nucleocytoplasmic transport. The observation that the NRS is active in human HeLa cells provided an opportunity to study NRS function by a biochemical approach. The presence of 5′ and 3′ splice site-like sequences within the NRS implicated components of the splicing apparatus in NRS-mediated splicing inhibition. By using HeLa nuclear extracts, it was shown that the NRS inhibits in vitro splicing of model pre-mRNAs and that the spliceosomal small nuclear ribonucleoprotein particles (snRNPs) U1 and U2, which bind 5′ and 3′ splice sites, respectively, interact with the NRS (19). Two other snRNPs that seem to replace U1 and U2 for splicing of a rare class of mRNAs, U11 and U12 (20), also bind the NRS in vitro and seem to be required for function because mutations which abrogate binding of these snRNPs abolish NRS activity (19). The interaction of these additional snRNPs, and possibly other proteins, with the NRS was reflected in the formation of abnormally large ribonucleoprotein complexes on NRS-containing pre-mRNAs (19).

In an effort to dissect further the mechanism of NRS splicing inhibition and address the notion that it functions through non-snRNP host proteins, we have used nuclear extracts and assays to detect protein-RNA interactions to identify cellular *trans*-acting factors that bind the element. A minimum of four proteins in HeLa nuclear extracts were shown by UV cross-linking to interact specifically with the NRS (p26, p36, p44, and p55). One of them, p55, was also detected in complexes identified by an electrophoretic mobility shift assay (EMSA). The other three NRS-binding proteins have biochemical properties similar to those of SR protein splicing factors, and a number of purified SR proteins interact specifically with the NRS but not with nonfunctional mutants or nonspecific RNAs. The major cross-linking species appears to be the splicing factor SF2/ASF. In light of these findings, it appears that RSV has evolved a mechanism to block splicing that involves proteins critical for that very process.

MATERIALS AND METHODS

Plasmid constructions and in vitro RNA transcription. Viral DNA fragments were obtained from pAPrC (33), a proviral clone of the Prague-C strain of RSV; sequence coordinates are as described by Schwartz et al. (37). p3ZXS was made by inserting an *Xho*I-*Sph*I fragment (nt 631 to 1011) into the *Sal*I-*Sph*I sites of pGEM-3Z (Promega). This plasmid was digested with *Bam*HI and *Mro*I, blunt ended, and recircularized to produce p3ZMS, which contains RSV nt 707 to 1011. A blunt-ended *Bst*NI fragment (nt 703 to 930) was cloned in the *Sma*I site of pGEM-3Z in the sense orientation to generate p3ZBB. p3ZBB5′ was generated by PCR amplification (35) with a sense primer containing an engineered *Kpn*I site and RSV sequences from nt 701 to 715 and an antisense primer containing an engineered *Xba*I site and nt 783 to 797, and the PCR fragment was cloned into *Kpn*I-*Xba*I-digested pGEM-3Z. By a similar strategy, p3ZBB3′ was made with sense primer 798-812 (containing nt 798 to 812) and antisense primer 919-932 and p3ZBBΔ715 was made with sense primer 715-729 and antisense primer 919-932. p3Z776-Sph was made with sense primer 776-790 and antisense primer 988-1011. pKS-XSΔ748 was made by ExoIII-mung bean deletion (21) of pKSXS, which had an *Xho*I-*Sph*I RSV fragment (nt 631 to 1011) inserted into the *Sal*I-*Sph*I sites of pBluescriptII KS(+) (Stratagene). In vitro transcription reactions (32) were performed with [^{32}P]UTP and T7 RNA polymerase, as described previously (19), and the following cut vectors: *Pvu*II-cut pGEM-4Z, *Bst*NI-cut pBluescriptII KS(+), *Hin*dIII-cut p3ZMS (MS RNA), *Bam*HI-cut p3ZBB (BB RNA), *Xba*I-cut p3ZBB3′ (BB3′ RNA), *Xba*I-cut p3ZBB5′ (BB5′ RNA), *Xba*I-cut p3ZBBΔ715 (BBΔ715 RNA), *Bst*NI-cut p3Z777-Sph (BBΔ776 RNA), and *Bst*NI-cut pKS-XSΔ748 (BBΔ748 RNA). Transcripts contained 16 to 21 nt of vector sequences at their 5′ ends and a maximum of 4 nt at the 3′ ends (Fig. 1). All RNAs were gel purified, and identical results were obtained with capped and uncapped RNAs.

As with other NRS fragments, the BBΔ715 fragment was tested for splicing inhibition in vivo as described previously by being inserted into the intron of pRSVNeo-int (31). DNA was transfected into HeLa cells, and the RNA harvested 40 h later was used in an RNase protection assay with a probe spanning the 5′ splice site to monitor the steady-state levels of unspliced and spliced RNA simultaneously. The BBΔ715 fragment was as inhibitory as the parental BB fragment, resulting in more than 70% unspliced RNA (data not shown). No inhibition was seen when the fragment was in the antisense orientation.

Preparation of proteins. HeLa S3 cells were grown in spinner cultures in RPMI 1640 medium containing 7% bovine calf serum (Bethesda Research Laboratories). Nuclear and S100 extracts were prepared as described previously (11). To prepare the 0 to 50% and 50 to 80% ammonium sulfate fractions, 1 ml of nuclear extract was diluted with 1.5 ml of 20 mM HEPES (*N*-2-hydroxyethylpiperazine-*N*′-2-ethanesulfonic acid; pH 8.0)–0.2 mM EDTA–1 mM dithiothreitol (DTT), an equal volume of saturated $(NH_4)_2SO_4$ was added, and the mixture was stirred on ice for 1 h. Insoluble material was pelleted for 30 min at 4°C at 5,300 rpm in an HB6 rotor (Sorvall). The supernatant was removed to a new vessel, and solid $(NH_4)_2SO_4$ was added to 80% with stirring on ice. This solution was spun as before, and each pellet was dialyzed against 20 mM HEPES (pH 8.0)–0.1 M KCl–5% glycerol–0.2 mM EDTA–1.0 mM DTT–0.5 mM phenylmethylsulfonyl fluoride. Total HeLa cell SR proteins were prepared exactly as described previously (46). JM101 bacterial cells harboring an expression vector for a histidine-tagged ASFΔRS protein was obtained from J. Manley, and the protein was produced from inclusion bodies by Ni^{2+} affinity chromatography (His-Bind Resin; Novagen) essentially as described previously (48). The protein was eluted with 0.5 mM imidazole and dialyzed against 20 mM HEPES (pH 7.9)–42 mM $(NH_4)_2SO_4$–15% glycerol–0.5 mM DTT–0.2 mM EDTA–0.5 M guanidine-HCl at 4°C. Insoluble material was removed by centrifugation, and aliquots were stored at −80°C. ASFΔRS protein was diluted appropriately in storage buffer just prior to addition to reaction mixtures. All protein concentrations were determined by the Bradford method (7) with a kit from Bio-Rad.

UV cross-linking and EMSAs. For UV cross-linking assays with nuclear and

S100 extracts, 100,000 to 300,000 cpm (3 to 5 fmol) of RNA was incubated for 30 min at 30°C under in vitro splicing conditions (20 mM HEPES [pH 7.9], 33 mM KCl, 3.2 mM $MgCl_2$, 0.15 mM DTT, 6% glycerol [16]) in the absence or presence of 0.5 mM ATP–20 mM creatine phosphate as specified in the figure legends, in a 25-μl volume containing 33% extract or the indicated amount of protein. For SR proteins and recombinant ASFΔRS, the binding buffer was 10 mM HEPES (pH 7.9)–200 mM KCl–20 mM NaCl–0.025% Nonidet P-40–1 mM DTT–15 μg of bovine serum albumin per ml–10% glycerol (48), and 2 μg of SR protein or 20 pmol of ASFΔRS was used. For competition studies, labeled and unlabeled RNAs (amounts are indicated in the figure legends) were added simultaneously to the extract or protein preparations. Reaction mixtures were then subjected to UV cross-linking for 20 min at 4°C using 254-nm light from a UVP model UVG-54 lamp at a distance of 4 cm. RNase A was added to 1 mg/ml, and samples were incubated at 37°C for 15 min, at which point an equal volume of 2× sample buffer was added and the reaction mixtures were analyzed by sodium dodecyl sulfate-polyacrylamide gel electrophoresis (SDS-PAGE) (26). After Coomassie staining to locate size standards, the gels were dried and autoradiography was performed.

Binding conditions for EMSAs were similar to those described for extract cross-linking except that KCl was at 70 mM, 1 μg of tRNA was included, and only 5 μg of protein was used. After heparin was added to 5 mg/ml, the samples were incubated at 30°C for 10 min and run on a 4% nondenaturing polyacrylamide gel (acrylamide/bisacrylamide ratio, 29:1) at room temperature at ~12 V/cm. Gels were dried and autoradiography was performed. For elution experiments, the wet gels were irradiated with UV light as described above and the complexes were located by autoradiography at 4°C. Complexes from four replicate lanes were cut out and treated for 1 h at 37°C with 1 mg of RNase A per ml in 10 mM Tris-HCl (pH 7.9)–10 mM $MgCl_2$. The RNase solution was removed, and elution was carried out on a nutator for 24 h at 4°C in a solution containing 0.1% SDS, 50 mM Tris-HCl (pH 7.9), 0.1 mM EDTA, 5 mM DTT, and 150 mM NaCl. Gel fragments were removed by centrifugation, and the samples were concentrated by acetone precipitation. Pellets were resuspended in sample buffer and subjected to SDS–12% PAGE and autoradiography. Proteinase K-treated samples were incubated with 50 μg of proteinase K per ml at 37°C for 20 min prior to electrophoresis.

Immunoprecipitations. BB RNA labeled with [^{32}P]UTP and [^{32}P]GTP was incubated for 20 min at room temperature under splicing conditions (50 μl) in the absence of ATP and cross-linked as described above. Reaction mixtures were diluted to 650 μl with IP buffer (50 mM Tris-HCl [pH 7.8], 150 mM NaCl, 0.05% Nonidet P-40) and cleared with a nonspecific mouse monoclonal antibody linked to protein A-agarose (ICN Biomedicals, Inc.). The cleared reaction mixtures were added to SF2 monoclonal antibody (kindly provided by A. Krainer) or control mouse monoclonal antibody to mouse myelin basic protein that had been prebound to protein A-agarose, and the samples were nutated overnight at 4°C. Bound material was washed six times with 1 ml of IP buffer and then eluted in SDS-PAGE sample buffer at 85°C for 10 min. Protein A-agarose beads were removed by centrifugation, and the samples were subjected to SDS-PAGE in a 12% gel. The gel was stained to locate size standards and dried, and autoradiography was performed.

RESULTS

UV cross-linking of HeLa nuclear proteins to the NRS. UV cross-linking assays were initially used to determine if factors present in nuclear extracts could specifically interact with the NRS. When reaction mixtures are exposed to UV light, covalent cross-links may be induced between proteins and labeled RNA if the two are in contact, resulting in protein labeling. Since it had been shown previously that the NRS could block in vitro splicing of an adenovirus pre-mRNA, in vitro splicing conditions were chosen for the protein binding step to mimic a functional environment. Figure 1 shows the NRS substrates used in this study, their positions in RSV, and relative inhibitory activities determined from in vivo splicing inhibition assays (31). The inhibitory activity of BBΔ715 was determined for this study.

UV cross-linking reactions were carried out with ^{32}P-labeled BB RNA and various amounts of nuclear extract in the presence and absence of ATP (Fig. 2). In the presence of ATP, labeled proteins were detected when 5 μg of extract protein was used. Band intensity increased and additional bands appeared when 25 μg of protein was used, and the pattern did not change appreciably when up to 100 μg was used (lanes 1 to 5). One protein at ~116 kDa disappeared when more than 5 μg of protein was used (lane 2), and a species at ~42 kDa was either lost or obscured by a smear of labeled protein. The major

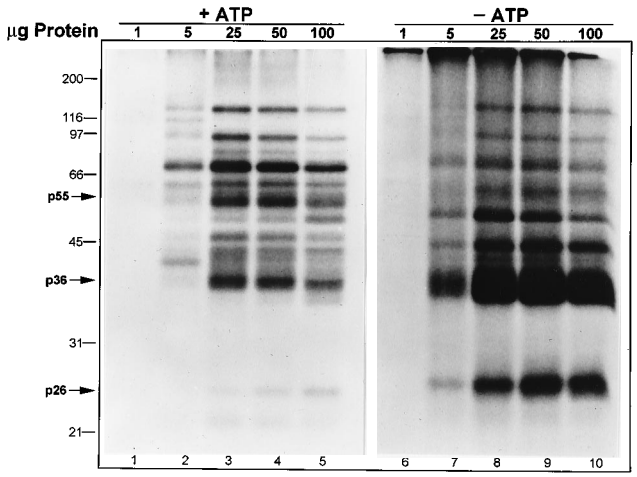

FIG. 2. UV cross-linking of HeLa nuclear proteins to the NRS. [^{32}P]UTP-labeled NRS RNA derived from a 231-base *Bst*NI (BB) fragment was incubated under in vitro RNA splicing conditions with the indicated amounts of nuclear extract protein in the presence or absence of ATP, and UV cross-linking was carried out as described in Materials and Methods. Samples were resolved by SDS-PAGE on a 12% gel, and autoradiography was performed. The positions of the 26-, 36- and 55-kDa NRS-binding proteins and molecular mass markers (in kilodaltons) are indicated; p44 was not obvious in this experiment. Both panels are from the same gel, and the left panel exposure was three times longer than that for the panel on the right.

cross-linked species had molecular masses of 135, 94, 72, 55, 36, and 26 kDa; the latter two often appeared as doublets. The cross-linking pattern was somewhat different when binding reactions were performed without ATP (lanes 6 to 10). Band intensities were generally much stronger at the same exposure at all protein concentrations, and maximal cross-linking was again achieved with 5 to 25 μg of protein. The most prominent bands comigrated with the 36- and 26-kDa bands observed in the presence of ATP. The 55-kDa protein either does not cross-link to BB RNA in the absence of ATP or is obscured by a smear in that region. We favor the latter explanation, since the 55-kDa protein was present in complexes identified by EMSA (see below). All the labeled bands were attributed to proteins, since none appeared when UV irradiation was omitted or when cross-linked samples were treated with proteinase K prior to electrophoresis (data not shown). Thus, under these conditions a number of proteins in nuclear extract cross-link to the NRS.

To assess the cross-linking specificity of the proteins detected in the experiment for Fig. 2, an additional NRS substrate and a nonspecific RNA derived from pGEM-4Z vector sequences were employed. As shown in Fig. 3A, the longer version of the NRS (MS RNA [lane 3]) produced an array of cross-linked proteins similar to that produced by BB RNA (lane 2 and Fig. 2). MS RNA consistently showed more prominent cross-linking to the 55-kDa protein than did BB RNA, whose cross-linking to this protein was variable (compare lane 3 with lane 2; Fig. 4). Vector RNA derived from pGEM (lane 1) produced a pattern similar to that produced by NRS RNA except for the absence of the 55-kDa protein (called p55) and the presence of more intense cross-linking to a 72-kDa protein. The absence of p55 cross-linking to nonspecific RNA suggested that p55 was the major NRS-binding protein. These results did not rule out the possibility that p55 interacted with vector RNA but merely cross-linked inefficiently.

Binding specificity of nuclear proteins for the NRS was investigated further by examining the abilities of 50-, 250-, and

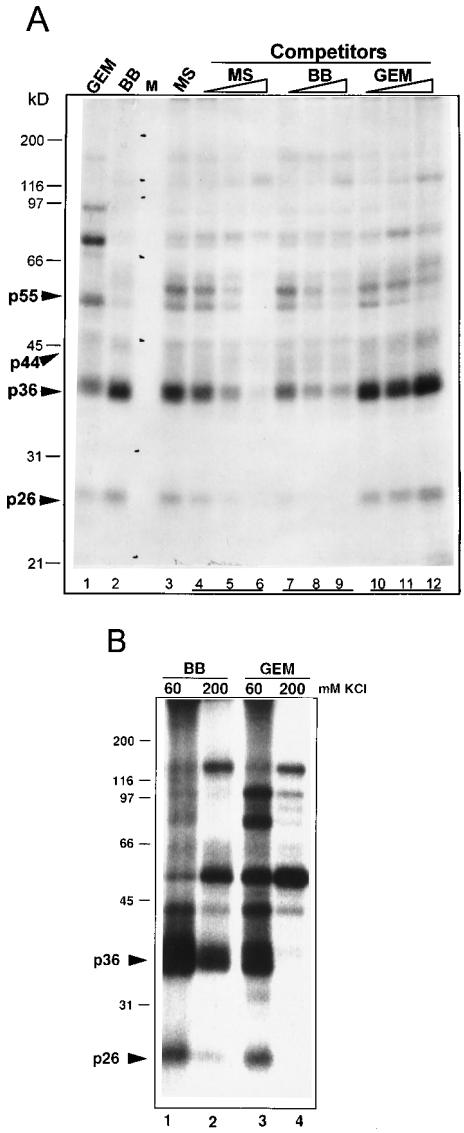

FIG. 3. Specific cross-linking of HeLa nuclear proteins to the NRS. (A) UV cross-linking was performed on binding reaction mixtures incubated under in vitro splicing conditions (in the presence of ATP) with nuclear extract and labeled nonspecific RNA derived from vector sequences (GEM [lane 1]), or NRS RNAs from *Bst*NI (BB [lane 2]) or *Mro*I-*Sph*I (MS [lane 3]) fragments, and the reaction mixtures were resolved by SDS–12% PAGE. Competitions were performed with 50-, 250-, and 750-fold molar excesses of unlabeled MS, BB, or GEM RNA as indicated by the wedges (lanes 4 to 12). Unlabeled RNAs were added at the same time as was labeled MS RNA. Molecular mass markers were loaded between lanes 2 and 3 (lane M) and visualized by staining before autoradiography. The positions of p26, p36, p44, p55, and molecular mass markers are indicated on the left. (B) The UV cross-linking assay was carried out on reaction mixtures incubated as described for panel A with BB NRS or GEM RNA as indicated and either 60 mM KCl (lanes 1 and 3) or 200 mM KCl (lanes 2 and 4). The image in panel B was acquired by scanning the autoradiogram with Adobe Photoshop, and the photograph was produced with Microsoft Powerpoint software.

750-fold molar excesses of unlabeled BB, MS, and pGEM RNA to compete with labeled MS RNA for protein cross-linking (Fig. 3A). As expected, unlabeled MS RNA was a very efficient competitor (lanes 4 to 6), but even at the highest concentration cross-linking of some proteins remained unchanged or even increased (lane 6). BB RNA also effectively competed for cross-linking with some but not all proteins, and its competition closely resembled that seen with unlabeled MS RNA (lanes 7 to 9). Despite cross-linking inefficiently to p55, BB RNA still competed strongly for p55 cross-linking, indicating that p55 readily binds both NRS RNAs but cross-links inefficiently to BB RNA. In contrast to the results obtained with the NRS competitors, pGEM RNA failed to compete for p55 binding (lanes 10 to 12), and this argues against the possibility that p55 interacted with pGEM RNA but cross-linked inefficiently, as was the case for BB RNA. Surprisingly, the nonspecific RNA also failed to compete for binding of a number of other proteins, including p26, p36, and a minor smear of approximately 44 kDa, despite its ability to cross-link to them with the same efficiency as the NRS RNAs (lanes 1 to 3). The lack of competition by pGEM was not general, since a number of other proteins were effectively inhibited. It should be noted that these binding conditions are not stringent, since the reaction mixtures contain relatively low salt concentrations (33 mM KCl). Low-affinity RNA binding in these experiments would not be suppressed and would explain why pGEM sequences could cross-link but not compete for protein binding. In fact, when the KCl concentration was raised to 200 mM, p26 and p36 cross-linking to pGEM RNA was much reduced compared with that of BB RNA, whereas other proteins cross-linked equally well (Fig. 3B; compare lanes 2 and 4).

The results of the reciprocal competition experiment in which BB RNA was labeled are shown in Fig. 4. The results from the cross-linking-only reactions (lanes 1 and 2) are consistent with those shown in Fig. 3A; p26, p36, and the 44-kDa protein were observed, and p55 cross-linking to BB RNA was again weak but detectable. The competition patterns generated with unlabeled BB RNA (lanes 3 to 5) and MS RNA (lanes 6 to 8) were almost identical, and competition for p55 binding was evident. In addition, competition for cross-linking

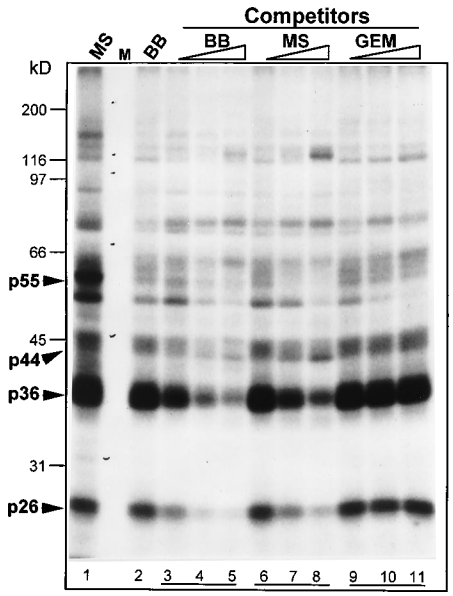

FIG. 4. Competitions demonstrate specificity of protein cross-linking to BB NRS RNA. UV cross-linking assays were performed as for Fig. 3 with nuclear extract and labeled MS or BB NRS RNAs (lanes 1 and 2). For competition studies, labeled BB RNA was incubated with 50-, 250-, and 750-fold molar excesses of the indicated unlabeled RNAs as indicated by the wedges (lanes 3 to 11). Reaction mixtures were subjected to electrophoresis on an SDS–12% polyacrylamide gel which was stained and destained prior to autoradiography. Molecular mass markers were run between lanes 1 and 2. The positions of p26, p36, p44, and p55 are indicated on the left. p55 cross-linking to BB RNA is weak but evident. The appearance of p44 was particularly clear in this experiment.

of the p26, p36, and the ~44-kDa proteins by each unlabeled NRS RNA was observed (lanes 3 to 5 and 6 to 8), and as before, pGEM did not compete (lanes 9 to 11). Thus, in addition to strict binding specificity seen for p55, we conclude from the competition studies that p26, p36, and minor cross-linking proteins of ~44 kDa demonstrate strong preferential binding to the NRS. Binding of one or more of these proteins to the NRS may be of functional relevance.

Detection of a 55-kDa protein in specific complexes by an EMSA. EMSAs were also performed to detect nuclear extract proteins that interact with the NRS. When complexes were formed by using the binding conditions for UV cross-linking and ~5 μg of nuclear extract protein, two specific complexes were formed on BB RNA (Fig. 5A; compare lanes 1 and 2) but not on pGEM RNA (data not shown). The second, diffuse complex of slower mobility (complex II) was barely visible at this exposure. Similar results were obtained when reaction mixtures lacked ATP (data not shown). Complex formation was reduced by a 25-fold molar excess of unlabeled BB RNA, and the competition was virtually complete when a 100-fold excess was used (lanes 3 to 6). No competition was seen with pGEM RNA (lanes 7 to 10). A more rapidly migrating complex was seen when NRS competitor was included in the binding reactions, and its intensity was proportional to the amount of competitor added (lanes 3 to 6). This complex may represent a different conformer of free RNA or a nonspecific complex resulting from titration of specific NRS-binding proteins by unlabeled NRS RNA. The fast-migrating complex was not observed in abundance when pGEM RNA was used as a competitor. Instead, a second complex of slower mobility that is only faintly seen in the absence of competitor was observed. This suggests that multiple proteins bind to lower-affinity sites that are made available when nonspecific proteins are titrated by pGEM competitor RNA. Regardless of the nature of the secondary complexes observed in the presence of competitor RNA, the results are significant in that the complexes are specific to the NRS and might be related to the factors identified in the cross-linking studies. To roughly determine the sequences required for the shift, reactions were done with the NRS 5′- and 3′-half substrates (Fig. 5B). Clearly, the 5′ substrate was very efficiently shifted, whereas the 3′ substrate showed no shift at all (lanes 5 and 6). It can be concluded that nuclear NRS-binding factors detected by EMSA bind preferentially to the purine-rich 5′ half of the NRS.

To determine whether any of the NRS-binding proteins observed by UV cross-linking were present in the EMSA complexes identified above, a mobility shift assay was performed and the gel was irradiated with UV light to induce cross-links within the complex. RNA-protein complexes were then located by autoradiography and cut out of the wet gel, and the eluted components were subjected to SDS-PAGE and autoradiography. As shown in Fig. 6, a broad band at ~55 kDa was detected only when complexes were exposed to UV light (lanes 1 and 2). The signal was attributed to protein and not residual RNA, since it was not seen when samples were treated with proteinase K prior to electrophoresis (lane 3) or when a gel slice containing labeled RNA was processed (lane 4). The 55-kDa protein could also be eluted from the more slowly migrating complexes produced in the presence of competitor pGEM RNA and from the complexes formed on BB5′ RNA (data not shown). However, even upon very long exposures p26, p36, and p44 were not detected in these experiments. The binding of these proteins may not be stable under the mobility shift gel conditions, possibly because of the heparin treatment used to suppress nonspecific protein binding, and this may be the reason why only p55 was detected. Heparin treatment has been

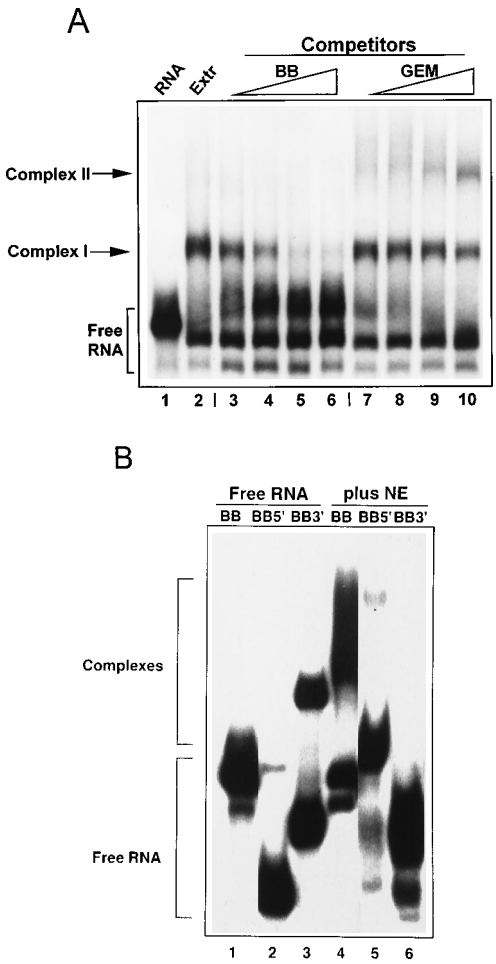

FIG. 5. Specific complexes are detected on NRS RNA in nuclear extract by EMSA. (A) ^{32}P-labeled BB RNA was incubated with ATP under in vitro splicing conditions in buffer (lane 1) or in the presence of nuclear extract (Extr) (lanes 2 to 10), heparin was added to 5 mg/ml, reaction mixtures were run on a 4% nondenaturing polyacrylamide gel (acrylamide/bis ratio, 29:1), and autoradiography was performed. For competitions, labeled BB RNA was incubated with 25-, 50-, 100-, and 250-fold molar excesses of unlabeled BB RNA (lanes 3 to 6) or GEM RNA (lanes 7 to 10) as indicated by the wedges. The positions of free RNA and the two NRS complexes are indicated on the left. (B) Binding reactions were done with BB, BB5′, and BB3′ RNA in buffer (lanes 1 to 3) or nuclear extract (NE; lanes 4 to 6) and subjected to EMSA as described in panel A . The gel-purified BB3′ RNA ran as two bands on the nondenaturing gel (lane 3); heating the RNA before addition to reactions eliminated the upper band, but still no complexes were formed in nuclear extract. The image in panel B was acquired by scanning the autoradiogram with Adobe Photoshop, and the photograph was produced with Microsoft Powerpoint software.

shown to disassemble spliceosomes in similar native gels (34). The striking specificity seen by cross-linking and detection of p55 within complexes specifically formed on the NRS suggests but does not prove that binding of this protein is functionally significant.

SR protein splicing factors bind the NRS. The NRS-binding proteins identified above are similar in size to members of the SR protein family of splicing factors (13, 46). The major SR proteins of ~20, 30, 40, and 55 kDa would be expected to shift up in size to that observed for the NRS-binding proteins after cross-linking to RNA. Since SR proteins are present in nuclear extract but absent from the S100, we sought to determine by UV cross-linking if any of the NRS-binding proteins fractionated similarly. As shown in Fig. 7 with MS RNA, p26 and p36

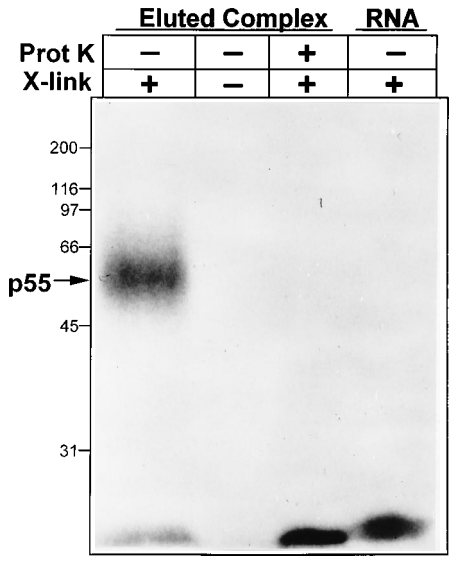

FIG. 6. A 55-kDa protein is present in complexes resolved by EMSA. Reaction mixtures containing ^{32}P-labeled BB RNA and nuclear extract were subjected to EMSA, and the region of the gel containing the NRS complexes was irradiated with UV light where indicated (X-link plus) to induce cross-links in situ. NRS complexes located by autoradiography at 4°C were excised from the gel and treated with RNase A, and components of the complex were eluted by nutation overnight at 4°C. After combination of four eluted samples and concentration by acetone precipitation, samples were run on an SDS–12% polyacrylamide gel and autoradiography was performed. The sample in one set of controls was treated with proteinase K (Prot K) prior to electrophoresis. Gel slices from another control set containing free RNA rather than NRS complexes (RNA lane) were taken through the protocol in parallel with the other samples. The positions of molecular mass markers (in kilodaltons) and the 55-kDa protein are shown.

were clearly present in the nuclear extract (lane 1) but not the S100 (lane 2). A small amount of p55 was reproducibly detected in the S100, and the distribution of p44 could not be resolved. Since SR proteins precipitate into the high-salt pellet of nuclear extracts (46), we tested for the presence of NRS-binding proteins in the 0 to 50% and 50 to 80% ammonium sulfate pellets of nuclear extract. p55 was clearly present in the 0 to 50% pellet (lane 3), whereas p26, p36, and a 44-kDa protein were found in the 50 to 80% fraction (lane 4). Thus, while the data for p44 were less certain, the fractionation studies were consistent with the idea that p26 and p36, but not p55, are SR proteins.

Having shown that some of the proteins in nuclear extract which show preferential binding to the NRS possess biochemical properties similar to those of SR protein splicing factors, we purified total SR proteins from HeLa cells by the two-salt precipitation method of Zahler et al. (46) and used this preparation in UV cross-linking experiments. Figure 8A shows the quality of the SR protein-containing $MgCl_2$ pellet (lane 2) and supernatant from the pellet (lane 3). The supernatant proteins were largely excluded from the pellet, and vice versa, and characteristic SR proteins of 20, 30, 40, 55, and 75 kDa were obtained (designated SRp20, etc.). These proteins were also reactive with a monoclonal antibody (mAb 104) specific for a phosphoepitope present on SR proteins (reference 46 and data not shown). The results of a cross-linking experiment with a number of NRS RNAs and two nonspecific substrates are shown in Fig. 8B. When BB NRS RNA was used, cross-linking to all of the proteins but SRp75 was observed, with the signal from SRp30a/b being particularly intense (lanes 2 and 5). It is probably no coincidence that when the autoradiogram was superimposed on the dried gel, the radioactive signals were shifted upward relative to the stained proteins to the positions observed for the NRS-binding proteins in nuclear extract. In contrast to the results with BB RNA, little cross-linking was observed with nonspecific RNAs derived from pGEM (lane 1) or pBluescript (lane 8) sequences. The signal in the pGEM lane at ~26 kDa is largely due to an RNase A-resistant RNA fragment, since a band of similar intensity was observed in the absence of cross-linking (data not shown). A number of SR proteins interact with purine-rich sequences. To roughly localize the SR protein binding sites on the NRS, cross-linking was performed with the 5′ half of the NRS, which is particularly rich in purines, and the 3′ half, which is predominantly pyrimidines. Both halves are required but neither is sufficient for splicing inhibition (31). Clearly, the SR proteins cross-linked to the purine-rich 5′-half substrate but not to the 3′ half (compare lanes 3 and 4). Lanes 6 and 7 show cross-linking with BB RNAs truncated to nt 748 and 776 (Δ748 and Δ776), respectively. Neither of these RNAs cross-linked above the background level, whereas an RNA truncated to nt 715 (Δ715) cross-linked well (data not shown; see competitions described below). It appears that a number of SR proteins can interact with the purine-rich 5′ half of the NRS and that sequences between nt 715 and 748, which are important for inhibitory activity (Fig. 1), are required for cross-linking.

SF2/ASF binds the purine-rich region of the NRS. SRp30a/b, shown above to be the predominant SR protein that cross-linked to the NRS, is composed of at least two different proteins, SF2/ASF and SC35. These proteins possess similar in

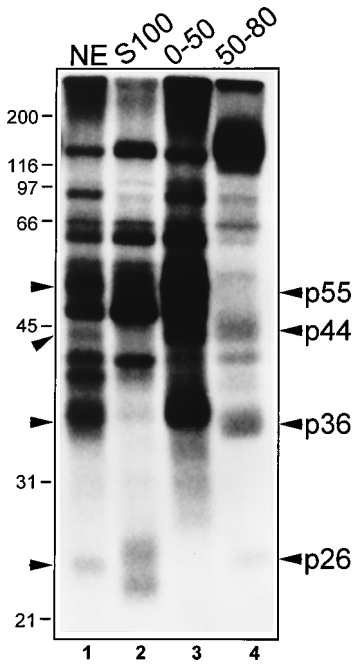

FIG. 7. Fractionation behavior of some NRS-binding proteins is characteristic of SR protein splicing factors. Labeled MS RNA was incubated under splicing conditions (in the presence of ATP) in 40 μg of either nuclear extract (NE) (lane 1), S100 extract (lane 2), or the 0 to 50% (lane 3) or 50 to 80% (lane 4) ammonium sulfate fraction of nuclear extract, and UV cross-linked samples were run on an SDS–12% polyacrylamide gel and processed for autoradiography. Some p55 was present in S100, but this protein was enriched in the 0 to 50% ammonium sulfate fraction, whereas p26 and p36 were excluded from the S100 and found in the 50 to 80% ammonium sulfate fraction. A 44-kDa protein was also enriched in the 50 to 80% pellet. Migration of molecular mass markers (in kilodaltons) is shown on the left, and the NRS-binding proteins are shown on the right.

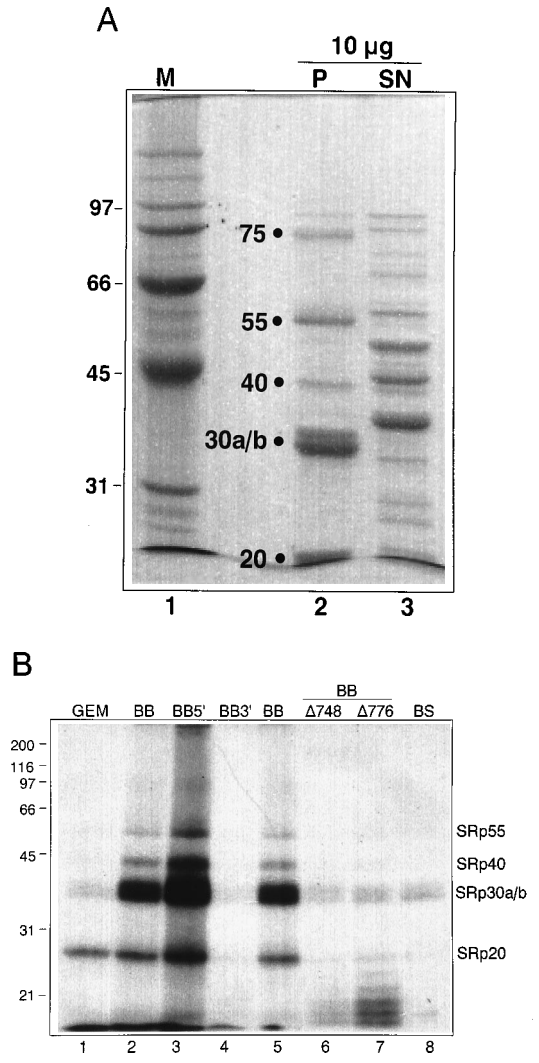

FIG. 8. SR protein splicing factors interact with the 5′ half of the NRS. (A) Total SR proteins were prepared from whole HeLa cells as described previously (46). Portions (10 μg) of protein from the SR protein-containing $MgCl_2$ pellet (P) and supernatant (SN) were visualized by SDS–10% PAGE and staining with Coomassie blue. Size standards were run in lane 1. (B) HeLa SR proteins were incubated with 100,000 cpm of RNA in binding buffer containing 200 mM KCl, and the UV cross-linking assay was performed. Control RNAs were from pGEM (lane 1) or pBluescript (lane 8), and NRS RNAs were BB RNA (lanes 2 and 5), BB5′ (lane 3), BB3′ (lane 4), BBΔ748 (lane 6), and BBΔ776 (lane 7). The low-molecular-weight bands at ~20 kDa in the Δ776 lane are RNA fragments. Images were acquired by scanning the autoradiogram with Adobe Photoshop, and photographs were produced with Microsoft Powerpoint software.

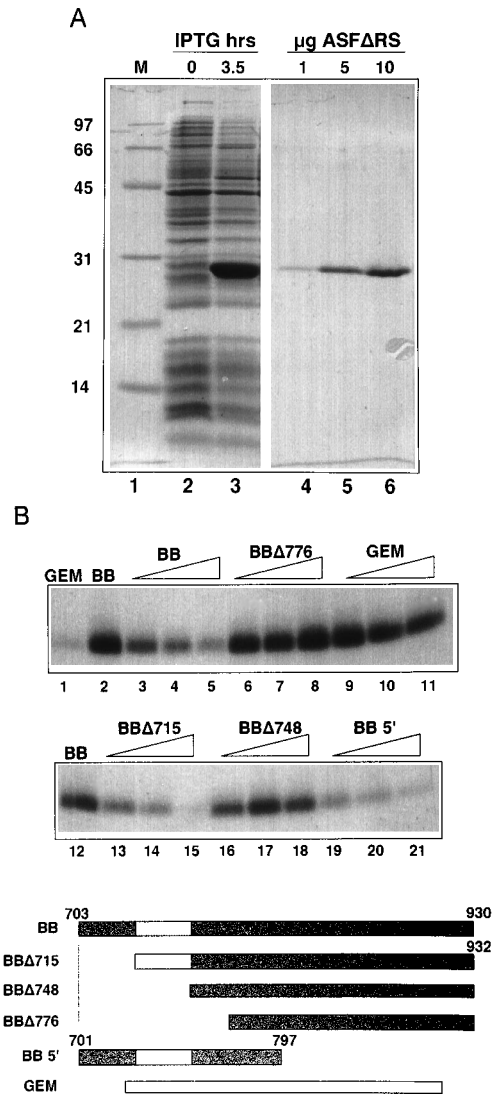

FIG. 9. Purified ASFΔRS binds purine-rich sequences in the 5′ half of the NRS. (A) A recombinant protein lacking the arginine-serine repeat domain, ASFΔRS, was expressed in bacteria and isolated from inclusion bodies by Ni^{2+} affinity selection. Shown is protein expression from aliquots of an uninduced culture (lane 2) and a culture induced with IPTG (isopropyl-β-D-thiogalactopyranoside) for 3.5 h (lane 3) that were lysed and run on an SDS–10% polyacrylamide gel. Lanes 4 to 6, from a different region of the same gel, show the patterns for 1, 5, and 10 μg of the final, purified ASFΔRS protein. M, markers. (B) Purified ASFΔRS (20 pmol) was incubated with labeled GEM RNA (lane 1) or BB RNA (lanes 2 and 12) or, for competitions, with labeled BB RNA and 50-, 100-, and 250-fold molar excesses of the indicated unlabeled RNAs, in 200 mM KCl binding buffer, and UV cross-linked samples were applied to an SDS–10% polyacrylamide gel and processed for autoradiography. The lower panel is a schematic of the RNAs used. RNAs are shown as shaded boxes with the internal open boxes depicting sequences required for ASFΔRS binding. The nonspecific GEM RNA is shown as an open box. Diagrams are not to scale. Images were acquired by scanning the autoradiogram with Adobe Photoshop, and photographs were produced with Microsoft Powerpoint software.

vitro biochemical properties (15) but display distinct binding specificities (44). In an effort to determine which protein was responsible for the observed SRp30a/b cross-link, we used a bacterially expressed SF2/ASF protein in cross-linking competition assays with labeled BB RNA and a number of unlabeled competitor RNAs. SR proteins contain an N-terminal RNA binding domain and a C-terminal region rich in arginine-serine (RS) dipeptide repeats (hence the name SR proteins) (46). We chose an SF2/ASF recombinant which lacks the RS domain (ASFΔRS), since this domain is not required for RNA binding and reduces binding specificity (44, 48). The ASFΔRS protein preparation used in these experiments was about 95% pure (Fig. 9A). Binding reactions were carried out at an elevated salt concentration (200 mM KCl), and the results showed strong rASFΔRS cross-linking to the NRS (Fig. 9B, lanes 2 and 12) but not to pGEM sequences (lane 1). This specificity was also demonstrated by competition with unlabeled BB and pGEM RNAs; the vector sequences did not compete at a concentration at which BB RNA was an effective competitor (compare lanes 3 to 5 and 9 to 11). To augment the results seen

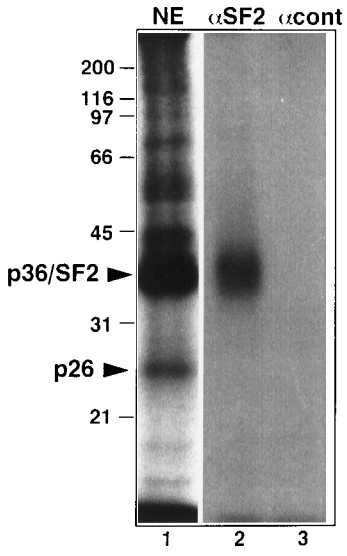

FIG. 10. SF2 monoclonal antibodies precipitate a cross-linked 36-kDa protein from nuclear extract. BB RNA labeled with [^{32}P]UTP and [^{32}P]GTP was incubated in nuclear extract under splicing conditions (with ATP) and cross-linked as described in Materials and Methods. Reaction mixtures were incubated overnight at 4°C with SF2 monoclonal antibody (αSF2) or an irrelevant monoclonal antibody (αcont), and immune complexes were pelleted with protein A-agarose, eluted, and subjected to SDS–12% PAGE. A control nuclear extract cross-linking reaction mixture that was not immunoprecipitated was run in lane 1 (NE). The three lanes are from the same gel, but lanes 2 and 3 were exposed 15 times longer than lane 1. Images were acquired by scanning the autoradiogram with Adobe Photoshop, and the photograph was produced with Microsoft Powerpoint software.

with total SR proteins, competitions were performed with the NRS 5′-half substrate and the BB truncations Δ715, Δ748, and Δ776. The 5′-half substrate and BBΔ715 were very effective competitors (lanes 19 to 21 and 13 to 15), whereas BBΔ776 and BBΔ748 were not (lanes 6 to 8 and 16 to 18). These results indicated that binding of ASFΔRS to the NRS is dependent on sequences between nt 715 and 748, in agreement with the results with total SR proteins. Significantly, the activity of NRS constructs Δ748 and Δ776 is severely impaired in vivo (31), while Δ715 is functional (Fig. 1). To ascertain if the 36-kDa band observed by cross-linking in nuclear extract was SF2/ASF, cross-linking reaction mixtures containing labeled BB RNA were immunoprecipitated with an SF2 monoclonal antibody to determine if cross-linked p36 could be specifically precipitated. As shown in Fig. 10, the SF2 antibody precipitated labeled SF2 and the mobility of this protein was indistinguishable from that of p36 seen in nuclear extract (lanes 1 and 2), while the control precipitation was negative (lane 3). No cross-linked p36 could be precipitated from S100 by the SF2 antibody (data not shown), in agreement with the above-presented results indicating that the S100 was devoid of p36. These data are strong evidence that p36 is SF2/ASF. The correlation between SR protein binding (possibly SF2/ASF alone) and NRS activity suggests that SR proteins play a prominent role in NRS-mediated splicing inhibition.

DISCUSSION

Retrovirus replication requires maturation of viral RNA transcripts through processing reactions carried out by the host cell RNA processing machinery. The nature of the viral life cycle requires that a substantial amount of the viral RNA remain unspliced and still be transported to the cytoplasm, which is not characteristic of cellular mRNAs in general. Complex retroviruses like human immunodeficiency virus and human T-cell lymphotropic viruses encode auxiliary proteins that can influence RNA metabolism to facilitate cytoplasmic accumulation of incompletely spliced RNA (10). Inefficient splicing and RNA transport in simpler viruses like RSV seem to be mediated by *cis*-acting RNA signals only rather than through an alteration of the splicing-transport apparatus by viral regulatory proteins. These viruses don't encode regulatory proteins, and viral RNAs are correctly processed even in the absence of viral protein synthesis (23, 41). Here, we report the identification of cellular proteins that may be involved in the maintenance of high levels of unspliced RSV RNA through interactions with a novel splicing inhibitor element, the NRS.

The results of UV cross-linking assays with HeLa nuclear extracts indicated that three proteins bind preferentially (p26 and p36) or exclusively (p55) to the NRS under in vitro splicing conditions. A fourth protein that cross-linked less intensely, p44, was observed in many experiments but was often obscured by a smear in that region. The preference of p26 and p36 binding for the NRS was not apparent initially, as equivalent signals were generated with NRS and nonspecific RNA. However, no competition was observed when nonspecific RNA was used, while both NRS RNAs were effective against each other. Specificity was more apparent in experiments conducted at higher salt concentrations, in which cross-linking to pGEM RNA was much reduced; it appears that these proteins have strong nonspecific RNA binding characteristics and that the NRS harbors a high-affinity site(s). EMSAs also indicated that a cellular protein(s) specifically interacts with the NRS. When NRS complexes within gel slices were cross-linked and the eluted proteins were resolved by SDS-PAGE, a labeled protein of approximately 55 kDa was identified. This was most likely the same protein observed in UV cross-linking experiments, but additional work is needed to establish this conclusion. The p55 binding site is within the 5′ half of the NRS, since the 5′-half substrate shifted very efficiently. It was somewhat surprising that p26 and p36, which cross-link well, were not detected by this approach. One explanation is that the heparin treatment used in these experiments, or the EMSA gel conditions, strips NRS complexes of these proteins, leaving only p55. Excess heparin has been shown to disassemble splicing complexes as assessed with native gels (34). It seems possible that the observed p55-containing complexes contained only a subset of the factors associated with an authentic NRS complex, the identification and characterization of which will require more gentle preparation procedures.

In view of a role for the NRS in splicing control, we considered the possibility that the NRS-binding proteins detected by UV cross-linking might be SR proteins, a family of structurally and functionally related essential splicing factors that include proteins of 20, 30, 40, 55, and 75 kDa (13, 46). One could imagine that the cross-linked NRS-binding proteins were SR proteins whose apparent molecular weights were shifted upward slightly by the tag of RNA remaining on the proteins in this procedure. Indeed, p26 and p36 were not found in the S100 extract and were fractionated into the high-salt pellet of ammonium sulfate-fractionated nuclear extract, which is characteristic of SR proteins (46). The data were less clear for p44, but a 44-kDa protein was enriched in the high-salt pellet. On the other hand, a portion of p55 was found in the S100 and the bulk was clearly in the 0 to 50% ammonium sulfate nuclear fraction, and thus p55 is not likely to be a classical SR protein. In a preparation of total SR proteins isolated from HeLa cells, all but SRp75 were reactive with NRS RNA and cross-linking of SRp30a/b (a doublet of two proteins, SF2/ASF and SC35)

was particularly strong. Significantly, the finding that bacterially expressed ASFΔRS was specific for the NRS and did not bind to nonfunctional NRS mutants indicates that this interaction may be of functional relevance. The isolated NRS 5′-half substrate that is rich in purines also bound ASFΔRS, and sequences between nt 715 and 748 were critical for binding and NRS activity; no binding was detected with the pyrimidine-rich 3′-half substrate. This is consistent with a recent report showing that SF2/ASF selects mainly purine-rich sequences in a selection-amplification protocol (44). While no perfect match to the reported SF2/ASF consensus sequence (RGAAGAAC or AGGACAGAGC) or to any of the individual winner sequences is present in the NRS, the sequence 719-GAGAAACC-726 matches at four of eight positions, and three of the mismatches are purines. The precipitation from nuclear extract of cross-linked p36 by anti-SF2 antibodies and the lack of specific cross-linking of baculovirus-expressed SC35 to the NRS (data not shown) are strong evidence that p36 is SF2/ASF. It is novel that this negative element might function through one or more essential splicing factors. A role for SF2/ASF in NRS function is consistent with studies showing that this protein functions in splice site switching and facilitates binding of U1 snRNP to 5′ splice sites (12, 17, 25, 48); U1 snRNP in fact binds the NRS (19). Interestingly, SF2/ASF was shown recently to inhibit simian virus 40 early pre-mRNA splicing in vivo (45), but no negative elements have thus far been reported to exist in this gene. Similar precipitation experiments are required to confirm our suspicion that p26 and p44 are SRp20 and SRp40, and more work is needed to determine if the factors can act singly or cooperatively.

An important future concern is to identify p55, which does not seem to be a classical SR protein but shows exquisite specificity for the NRS and potentially plays a role in its activity. It should be noted that additional SR proteins exist that do not copurify with the classical SR proteins (13). If involved in NRS activity, p55 may function in concert with SR proteins, since all but SRp75 bind the NRS 5′ half. p55 does not appear to be an snRNP component, since treatment of extracts with micrococcal nuclease, which disrupts snRNPs, had no effect on the protein cross-linking profile (data not shown). The U11 snRNP, whose binding to the NRS is important for activity (19), is refractory to MN treatment, but p55 is not likely to be a U11 snRNP protein since a 55-kDa protein was not among those recognized by serum specific for U11-U12 snRNP particles (18). Additional studies are needed to establish a correlation between p55 binding and NRS function.

How might the NRS work? The findings that the element binds snRNPs and interacts strongly with SR protein splicing factors suggest that it might be recognized as a 5′ or 3′ splice site and enter into dead-end (or transiently inhibitory) complexes with the authentic RSV 5′ or 3′ splice sites. In support of this notion, we have recently employed a gel filtration chromatography approach that has been used extensively to study a number of spliceosome-related complexes (34) and found that an ATP-independent complex does assemble on the NRS (9). Assembly of this complex is dependent on SR proteins and a micrococcal nuclease-sensitive factor(s) that is likely to be an snRNP. Moreover, a substrate containing the NRS and an isolated downstream 3′ splice site efficiently formed a complex in the presence of ATP, suggesting an interaction between factors bound to the NRS and the 3′ splice site. Alternatively, it is possible that the NRS itself represents a miniexon which serves to block splicing. Architecturally, the 3′ half of the NRS can be viewed as a miniexon, with a 3′ splice site-like region, a short space, and an uncommon 5′ splice site of the U11 class (20, 31). Interestingly, the intron of the *Drosophila* suppressor-of-white-apricot (SWAP) gene contains two copies of a negative element organized like a miniexon that is necessary for a splicing block in the presence of the regulatory protein, Dm-SWAP, which itself is related to splicing factors (38). The RSV case is somewhat different in that specialized proteins like SWAP are not required for regulation. Even if the NRS 3′ half represents a miniexon, it in itself is not sufficient for splicing control, as a contribution of the 5′ half of the NRS is required for activity (31). We speculate that the 5′ purine-rich sequences might serve an RNA splicing enhancer function, as recently described purine-rich splicing enhancers function through SR proteins, including SF2/ASF, and recruit U1 snRNPs (40, 43, 44). Experiments addressing this possibility are in progress.

Complex retroviruses like human immunodeficiency virus do not appear to contain elements with global activities similar to the NRS, since deletions throughout the genome fail to alter the ratio of unspliced RNA to spliced RNA (1, 30). However, a number of site-specific *cis*-acting positive and negative regulatory sequences have been described (1, 2, 39). The mechanism by which the human immunodeficiency virus Rev protein facilitates structural gene expression remains controversial, but it has been proposed to function in part through splicing inhibition (24); other data are consistent with a role at the level of RNA stabilization (36), RNA export from the nucleus (27), and translation in the cytoplasm (5). Recently, control of alternative splicing of equine infectious anemia virus RNA by the equine infectious anemia virus Rev protein has been demonstrated (28). These systems contrast with those of simple retroviruses in that virus-encoded regulatory proteins influence RNA processing events, whereas simple retroviruses such as RSV do not encode such proteins. Here, splicing control must be due to *cis*-acting RNA signals and host cell proteins alone. It is novel that some of the host factors that we propose to be important for NRS splicing inhibition could be the very proteins critical for the splicing process itself.

ACKNOWLEDGMENTS

We thank J. Manley for providing the ASFΔRS expression vector, A. Krainer for providing the SF2 monoclonal antibody, R. Fritz for control monoclonal antibodies, and X.-D. Fu for the gift of SC35 protein. We thank Craig Cook for critical reading of the manuscript.

This work was supported by Institutional Research Grant 170 from the American Cancer Society and the Cancer Center of the Medical College of Wisconsin, a grant from the R. D. & Linda Peters Research Endowment, and an NIH First Award to M.T.M. Some preliminary experiments that led to this work were supported by NIH grant CA48746 to Karen Beemon.

REFERENCES

1. **Amendt, B. A., D. Hesslein, L.-J. Chang, and C. M. Stoltzfus.** 1994. Presence of negative and positive *cis*-acting RNA splicing elements within and flanking the first *tat* coding exon of human immunodeficiency virus type 1. Mol. Cell. Biol. **14:**3960–3970.
2. **Amendt, B. A., Z.-H. Si, and C. M. Stoltzfus.** 1995. Presence of exon splicing silencers within human immunodeficiency virus type 1 *tat* exon 2 and *tat-rev* exon 3: evidence for inhibition mediated by cellular factors. Mol. Cell. Biol. **15:**4606–4615.
3. **Amendt, B. A., S. B. Simpson, and C. M. Stoltzfus.** 1995. Inhibition of RNA splicing at the Rous sarcoma virus *src* 3′ splice site is mediated by an interaction between a negative *cis* element and a chicken embryo fibroblast nuclear factor. J. Virol. **69:**5068–5076.
4. **Arrigo, S., and K. Beemon.** 1988. Regulation of Rous sarcoma virus RNA splicing and stability. Mol. Cell. Biol. **8:**4858–4867.
5. **Arrigo, S. J., and I. S. Y. Chen.** 1991. Rev is necessary for translation but not cytoplasmic accumulation of HIV-1 *vif*, *vpr*, and *env/vpu* 2 mRNAs. Genes Dev. **5:**808–819.
6. **Berberich, S. L., and C. M. Stoltzfus.** 1991. Mutations in the regions of the Rous sarcoma virus 3′ splice sites: implications for regulation of alternative

splicing. J. Virol. **65:**2640–2646.
7. **Bradford, M. M.** 1976. A rapid and sensitive method for the quantitation of microgram quantities of protein utilizing the principle of protein-dye binding. Anal. Biochem. **72:**248–254.
8. **Coffin, J. M.** 1990. Retroviridae and their replication, p. 1437–1500. *In* B. N. Fields and D. M. Knipe (ed.), Virology, 2nd ed. Raven Press, New York.
9. **Cook, C. R., and M. T. McNally.** Unpublished data.
10. **Cullen, B. R.** 1992. Mechanism of action of regulatory proteins encoded by complex retroviruses. Annu. Rev. Microbiol. **45:**219–250.
11. **Dignam, J. D., R. M. Lebovitz, and R. D. Roeder.** 1983. Accurate transcription initiation by RNA polymerase II in a soluble extract from isolated mammalian nuclei. Nucleic Acids Res. **11:**1475–1489.
12. **Eperon, I. C., D. C. Ireland, R. A. Smith, A. Mayeda, and A. R. Krainer.** 1993. Pathways for selection of 5′ splice sites by U1 snRNPs and SF2/ASF. EMBO J. **12:**3607–3617.
13. **Fu, X.-D.** 1995. The superfamily of arginine/serine-rich splicing factors. RNA **1:**663–680.
14. **Fu, X.-D., R. A. Katz, A. M. Skalka, and T. Maniatis.** 1991. The role of branchpoint and 3′ exon sequences in the control of balanced splicing of avian retrovirus RNA. Genes Dev. **5:**211–220.
15. **Fu, X.-D., A. Mayeda, T. Maniatis, and A. R. Krainer.** 1992. General splicing factors SF2 and SC35 have equivalent activities *in vitro*, and both affect alternative 5′ and 3′ splice site selection. Proc. Natl. Acad. Sci. USA **89:**11224–11228.
16. **Garcia-Blanco, M. A., S. F. Jamison, and P. A. Sharp.** 1989. Identification and purification of a 62,000-dalton protein that binds specifically to the polypyrimidine tract of introns. Genes Dev. **3:**1874–1886.
17. **Ge, H., P. Zou, and J. L. Manley.** 1991. Primary structure of the human splicing factor ASF reveals similarities with *Drosophila* regulators. Cell **66:**373–382.
18. **Gilliam, A. C., and J. A. Steitz.** 1993. Rare scleroderma autoantibodies to the U11 small nuclear ribonucleoprotein and to the trimethylguanosine cap of U small nuclear RNAs. Proc. Natl. Acad. Sci. USA **90:**6781–6785.
19. **Gontarek, R. R., M. T. McNally, and K. Beemon.** 1993. Mutation of an RSV intronic element abolishes both U11/U12 snRNP binding and negative regulation of splicing. Genes Dev. **7:**1926–1936.
20. **Hall, S. L., and R. A. Padgett.** 1994. Conserved sequences in a rare class of eukaryotic nuclear introns with non-consensus splice sites. J. Mol. Biol. **239:**357–365.
21. **Henikoff, S.** 1984. Unidirectional digestion with exonuclease III creates targeted breakpoints for DNA sequencing. Gene **28:**351–359.
22. **Katz, R. A., M. Kotler, and A. M. Skalka.** 1988. *cis*-acting intron mutations that affect the efficiency of avian retroviral RNA splicing: implications for mechanisms of control. J. Virol. **62:**2686–2695.
23. **Katz, R. A., and A. M. Skalka.** 1990. Control of retroviral RNA splicing through maintenance of suboptimal processing signals. Mol. Cell. Biol. **10:**696–704.
24. **Kjems, J., and P. A. Sharp.** 1993. The basic domain of Rev from human immunodeficiency virus type 1 specifically blocks the entry of U4/U6.U5 small nuclear ribonucleoprotein in spliceosome assembly. J. Virol. **67:**4769–4776.
25. **Krainer, A. R., A. Mayeda, K. Kozak, and G. Binns.** 1991. Functional expression of cloned human splicing factor SF2: homology to RNA-binding proteins, U1 70K, and *Drosophila* splicing regulators. Cell **66:**383–394.
26. **Laemmli, U. K.** 1970. Cleavage of structural proteins during the assembly of the head of bacteriophage T4. Nature (London) **227:**680–685.
27. **Malim, M. H., and B. R. Cullen.** 1993. Rev and fate of pre-mRNA in the nucleus: implications for the regulation of RNA processing in eukaryotes. Mol. Cell. Biol. **13:**6180–6189.
28. **Martarano, L., R. Stephens, N. Rice, and D. Derse.** 1994. Equine infectious anemia virus *trans*-regulatory protein Rev controls viral mRNA stability, accumulation, and alternative splicing. J. Virol. **68:**3102–3111.
29. **McNally, M. T., and K. Beemon.** 1992. Intronic sequences and 3′ splice sites control Rous sarcoma virus RNA splicing. J. Virol. **66:**6–11.
30. **McNally, M. T., and K. Beemon.** Unpublished observation.
31. **McNally, M. T., R. R. Gontarek, and K. Beemon.** 1991. Characterization of Rous sarcoma virus intronic sequences that negatively regulate splicing. Virology **185:**99–108.
32. **Melton, D. A., P. A. Krieg, M. R. Rebagliati, T. Maniatis, K. Zinn, and M. R. Green.** 1984. Efficient *in vitro* synthesis of biologically active RNA and RNA hybridization probes from plasmids containing a bacteriophage SP6 promotor. Nucleic Acids Res. **12:**7035–7056.
33. **Meric, C., and P.-F. Spahr.** 1986. Rous sarcoma virus nucleic acid-binding protein p12 is necessary for viral 70S RNA dimer formation and packaging. J. Virol. **60:**450–459.
34. **Michaud, S., and R. Reed.** 1991. An ATP-independent complex commits pre-mRNA to the mammalian spliceosome assembly pathway. Genes Dev. **5:**2534–2546.
35. **Saiki, R. K., D. H. Gelfand, S. Stoffel, S. Scharf, R. H. Higuchi, G. T. Horn, K. B. Mullis, and H. A. Erlich.** 1988. Primer-directed enzymatic amplification with a thermostable DNA polymerase. Science **239:**487–491.
36. **Schwartz, S., B. K. Felber, and G. N. Pavlakis.** 1992. Distinct RNA sequences in the *gag* region of human immunodeficiency virus type 1 decrease RNA stability and inhibit expression in the absence of Rev protein. J. Virol. **66:**150–159.
37. **Schwartz, D. E., R. Tizard, and W. Gilbert.** 1983. Nucleotide sequence of Rous sarcoma virus RNA. Cell **32:**853–869.
38. **Spikes, D. A., J. Kramer, P. M. Bingham, and K. Van Doren.** 1994. SWAP pre-mRNA splicing regulators are a novel, ancient protein family sharing a highly conserved sequence motif with the prp21 family of constitutive splicing factors. Nucleic Acids Res. **22:**4510–4519.
39. **Staffa, A., and A. Cochrane.** 1995. Identification of positive and negative splicing regulatory elements within the terminal *tat-rev* exon of human immunodeficiency virus type 1. Mol. Cell. Biol. **15:**4597–4605.
40. **Staknis, D., and R. Reed.** 1994. SR proteins promote the first specific recognition of pre-mRNA and are present together with the U1 small nuclear ribonucleoprotein particle in a general splicing enhancer complex. Mol. Cell. Biol. **14:**7670–7682.
41. **Stoltzfus, C. M.** 1988. Synthesis and processing of avian sarcoma retrovirus RNA. Adv. Virus Res. **35:**1–38.
42. **Stoltzfus, C. M., and S. J. Fogarty.** 1989. Multiple regions in the Rous sarcoma virus *src* gene intron act in *cis* to affect accumulation of unspliced RNA. J. Virol. **63:**1669–1676.
43. **Sun, Q., A. Mayeda, R. K. Hampson, A. R. Krainer, and F. M. Rottman.** 1993. General splicing factor SF2/ASF promotes alternative splicing by binding to an exonic splicing enhancer. Genes Dev. **7:**2598–2608.
44. **Tacke, R., and J. L. Manley.** 1995. The human splicing factors ASF/SF2 and SC35 possess distinct, functionally significant RNA binding specificities. EMBO J. **14:**3540–3551.
45. **Wang, J., and J. L. Manley.** 1995. Overexpression of the SR proteins ASF/SF2 and SC35 influences alternative splicing in vivo in diverse ways. RNA **1:**335–346.
46. **Zahler, A. M., W. S. Lane, J. A. Stolk, and M. B. Roth.** 1992. SR proteins: a conserved family of pre-mRNA splicing factors. Genes Dev. **6:**837–847.
47. **Zhang, L., and C. M. Stoltzfus.** 1995. A suboptimal 3′ splice site is necessary for efficient replication of Rous sarcoma virus. Virology **206:**1099–1107.
48. **Zou, P., and J. L. Manley.** 1994. The human splicing factor ASF/SF2 can specifically recognize pre-mRNA 5′ splice sites. Proc. Natl. Acad. Sci. USA **91:**3363–3367.